Structure of recombinant ricin A chain at 2.3 Å

DEBRA MLSNA, ARTHUR F. MONZINGO, BETSY J. KATZIN,
STEPHEN ERNST, AND JON D. ROBERTUS
Department of Chemistry and Biochemistry, University of Texas, Austin, Texas 78712

Abstract

The plant cytotoxin ricin is a heterodimer with a cell surface binding (B) chain and an enzymatically active A chain (RTA) known to act as a specific *N*-glycosidase. RTA must be separated from B chain to attack rRNA. The X-ray structure of ricin has been solved recently; here we report the structure of the isolated A chain expressed from a clone in *Escherichia coli*. This structure of wild-type rRTA has and will continue to serve as the parent compound for difference Fouriers used to assess the structure of site-directed mutants designed to analyze the mechanism of this medically and commercially important toxin. The structure of the recombinant protein, rRTA, is virtually identical to that seen previously for A chain in the heterodimeric toxin. Some minor conformational changes due to interactions with B chain and to crystal packing differences are described. Perhaps the most significant difference is the presence in rRTA of an additional active site water. This molecule is positioned to act as the ultimate nucleophile in the depurination reaction mechanism proposed by Monzingo and Robertus (1992, *J. Mol. Biol. 227*, 1136-1145).

Keywords: cytotoxin; ricin A chain; X-ray structure

A variety of higher plants and some bacteria contain ribosome inhibiting proteins or RIPs (Olsnes & Pihl, 1982; Lord et al., 1991). Class 1 RIPs are roughly 30,000 molecular weight *N*-glycosidases, which remove a single adenine from a conserved stem and loop sequence of rRNA (Endo & Tsurugi, 1988). This depurination inactivates the ribosome. Class 2 RIPs contain an enzyme homologous to class 1 RIPs, called the A chain. In addition class 2 RIPs are complexed to one or more cell surface binding proteins, which facilitate cell uptake. Because of this property, class 2 RIPs are potent cytotoxins. Many efforts have been made to harness the toxicity of RIPs to form therapeutic agents, particularly in the form of immunotoxins (Frankel, 1988; Vitetta & Thorpe, 1991).

Probably the most widely studied class 2 RIP is ricin, and it may be considered the model molecule for this large class. We have solved the structure of the heterodimeric ricin by X-ray diffraction (Montfort et al., 1987) and refined the structure to 2.5 Å resolution (Rutenber et al., 1991). The structure of both the A chain (Katzin et al., 1991) and the lectin B chain (Rutenber & Robertus, 1991) have been described in detail.

The A chain of ricin (RTA) is linked by a disulfide bond to the B chain (RTB). RTB binds to target cell surfaces via its lectin action, and the disulfide bond keeps RTA, the toxic moiety, tethered until it is taken up by endocytosis. The bond is reduced in the cell permitting enzyme action; it is known that the heterodimer is inactive against ribosomes. It would be useful to know if any conformational change occurs to RTA upon release from RTB, perhaps one that facilitates toxic enzyme action. The structure of A chain may also be useful in the design of more effective immunotoxins (Vitetta & Thorpe, 1991).

The gene for ricin A chain has been cloned from mRNA (Lamb et al., 1985) and from the plant genome (Halling et al., 1985). A chain expressed from recombinant sources will be referred to here as rRTA. There is interest in defining the mechanism of action of RTA or rRTA as a representative of the RIP enzyme class. A number of studies using site-directed mutagenesis of rRTA have been carried out to this end (Frankel et al., 1990; Ready et al., 1991). Because it is the A chain that is catalytically active, a complete understanding of the mutagenesis results will require reference to the rRTA crystal structure.

The rRTA derived from an *Escherichia coli* expression system has been crystallized (Robertus et al., 1987). In this

---

paper we report the X-ray structure and refinement of the rRTA molecule. This model has already served as the basis for the recent analyses of two site-directed mutants of rRTA by X-ray crystallography (Kim et al., 1992; Kim & Robertus, 1992).

Results and discussion

Crystallographic refinement

The area detector was used to collect 60,841 observations of 16,705 unique reflections to 1.9 Å resolution for native rRTA. Only data to 2.3 Å resolution were used in the refinement. It was felt that the intensities and the number of replicated measurements of the higher resolution data could not guarantee the accuracy of those reflections. There were 49,196 observations of 10,973 reflections to 2.3 Å. The R_{merge} was 4% based on intensities. In the hopes of observing any anomalous dispersion signal, data were collected over a hemisphere of reciprocal space for the $PtCl_4$ and Me-Hg-adenine derivatives. Over 100,000 observations were made for each with R_{merge} values of 8% and 6%, respectively. The potential derivatives proved to be of no value in rRTA phase determination; difference Patterson maps could not be unambiguously interpreted. Ultimately, difference Fourier maps using calculated phases from molecular refinement and amplitudes of the form $(F_{der} - F_{nat})$ confirmed that the crystals soaked in either heavy atom compound were so poorly occupied that they could not be used for phase determination.

Molecular replacement efforts began using the refined A chain (Rutenber et al., 1991) of the ricin heterodimer as an initial model. Searches were carried out using a variety of resolution ranges and radii of integration. Resolution ranged from 20 to 4 Å while the integration radii varied from 12 to 20 Å. All the rotation searches showed the same major peak, which was typically 1.5 times higher than any secondary peak.

The most significant rotation peak established the A chain orientation to begin translation searches. The search vectors were confined to a plane normal to b since the space group determined a displacement along b of 0.5. The model resulting from the translation solution underwent least-squares rigid body refinement using CORELS. The R factor for the ricin A chain model in the resulting orientation was 0.36 using reflections to 2.5 Å.

The oriented model was then subjected to refinement by the simulated annealing method using X-PLOR; after one round of refinement the R factor dropped to 0.22. Six additional rounds of refinement, including manual rebuilding as described in the Materials and methods, were carried out to adjust the structure. Data were extended to 2.3 Å resolution for the last two rounds. Table 1 shows the changes in a number of parameters over the course of refinement. These include the deviation

Table 1. *Statistics for rRTA refinement*[a]

| Model | R factor | Root mean square deviation from ideality | | Root mean square deviation from model 8 | | Phase shift |
		Bonds	Angles	Main	Side	
1	0.362	0.029	4.64	1.15	2.20	43.5
2	0.215	0.019	3.97	1.08	2.05	39.1
3	0.212	0.019	3.99	1.07	1.94	37.2
4	0.209	0.019	3.89	0.43	0.89	26.2
5	0.189	0.021	4.06	0.26	0.60	21.3
6	0.178	0.019	3.87	0.23	0.57	20.2
7	0.163	0.017	3.70	0.17	0.48	16.4
8	0.175	0.017	3.86	–	–	–

[a] Model 1 is ricin A chain fit into rRTA electron density; model 8 is the final refined structure. The phase shift refers to the differences between phases calculated for a given model and those from the final model, 8.

from standard bond lengths and angles at each round. Also included are the positional deviations of a given model from the final one, model 8, and the phase differences for each model from the final ones. The final R factor, from 5.0 to 2.5 Å resolution, was 0.18. When data from 10 to 2.3 Å are included, R = 0.21. The model includes 48 water molecules; its root mean square (RMS) deviations from standard bond lengths and angles are 0.017 Å and 3.86°, respectively.

Figure 1 shows sections of the initial 2.5-Å map, phased from the molecular replacement solution of ricin A chain and the final "no electron density" (NED [omit]) map (see Materials and methods). For comparison, the latter map is also at 2.5 Å. It is clear that the initial ricin A chain model produced quite good phases, although the refinement process did improve the quality to some extent. The quality of the initial map shows succinctly that the two structures must be very similar.

The rRTA protein

As described above, a molecular replacement solution was found for rRTA, and the ricin A test molecule was subsequently refined against crystallographic data. This showed that the overall structure of rRTA is very similar to ricin A chain as previously seen in the heterodimer structure (Katzin et al., 1991; Rutenber et al., 1991). Figure 2 and Kinemage 1 show the superposition of the two Cα backbones. The RMS deviation of Cα positions is 1.2 Å while side-chain atoms show an RMS deviation of 2.2 Å.

Both the amino and carboxy termini of A chain are known to be mobile in solution (Bushnev & Tonevitsky, 1989) and they exhibit different positions in the two crystals (Fig. 2). The conformation of the amino-terminus of rRTA is quite interesting. As shown by Edman analysis roughly one-third to one-half of bacterially expressed
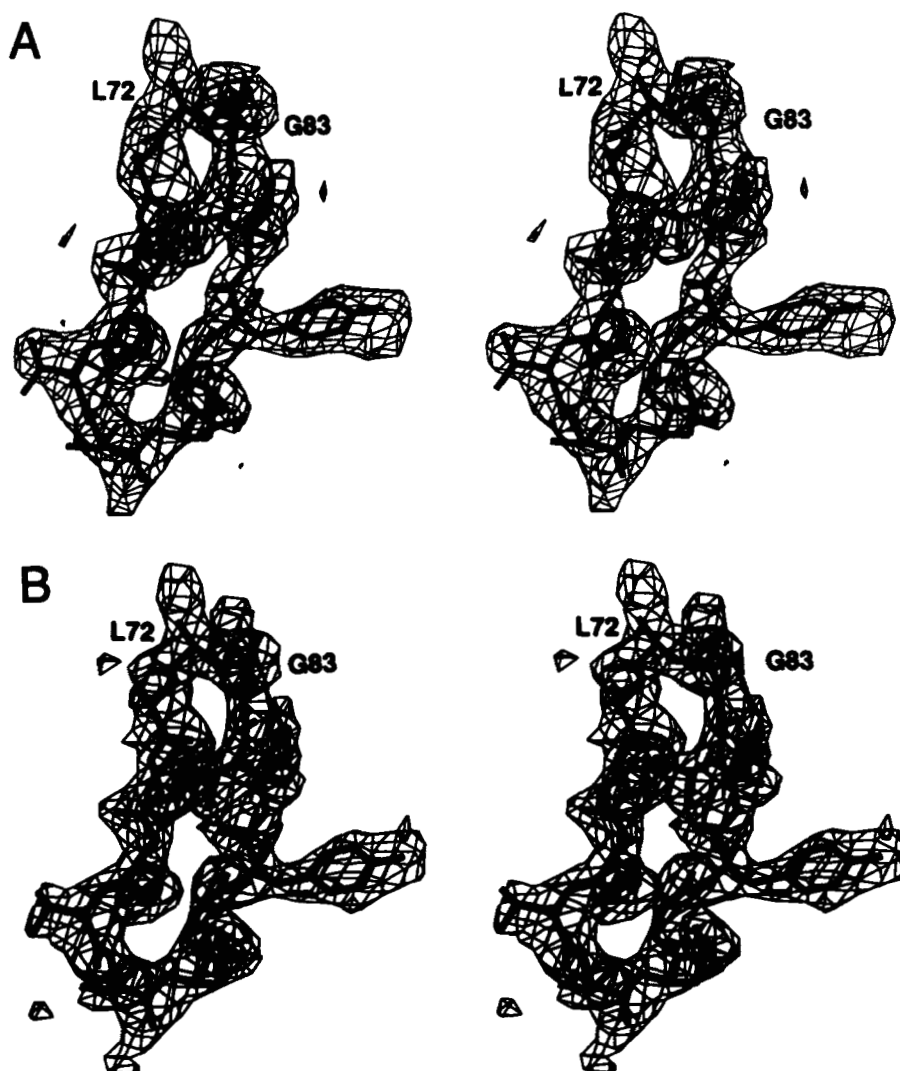
Fig. 1. Representative electron-density maps at the beginning and end of a recombinant ricin A chain (rRTA) refinement. In each stereo pair, residues 72–83 of the final refined protein model are superimposed on a 2.5-Å NED map (see text); the contour encloses 15% of the cell volume. **A:** The map based on ricin A chain oriented by CORELS; R = 0.40. **B:** The map corresponding to the final model; R = 0.18.

rRTA, and that from dissolved crystals, retains an unprocessed amino-terminal Met (Ready et al., 1991). The electron density maps have the additional density for Met 0 and it can be positioned readily. The Met side chain extends away from the body of the molecule, as indicated in Figure 2, where it contacts a hydrophobic pocket on a symmetry-related molecule. The pocket, formed by residues such as Tyr 183, Leu 207, Leu 132, Phe 240, and Ile 251, accommodates the side chain of Phe 262 from ricin B chain in the heterodimer. This is a part of the hydrophobic contacts that normally secure those two chains. The rRTA crystal packing adventitiously avails itself of this pocket to bind the Met 0 residue. Details of this interaction are shown in Figure 3. The conformation of the amino termini that do not contain Met 0 does not appear to be much different from those that do. The electron density for residues 1–4 is weak, suggesting some disorder, but there is no evidence of a major shift in chain position when the specific hydrophobic contact cannot be made.

As indicated in Figure 2, there are few significant differences in structure between the A chain of ricin and rRTA. One region with small, but real, differences is the loop region from residues 230–240. In the heterodimer, this is a region where A and B chain contact and where one might anticipate some changes when the chains separate. In ricin A chain this loop region was labeled as antiparallel strands g and h (Katzin et al., 1991). Although these strands resemble β structure the hydrogen-bonding pattern and ϕ, ψ angles deviated from ideal values (IUPAC, 1970) by an average of 41°. In the rRTA model this region becomes a standard antiparallel sheet with average deviations from ideality of only 24°. The readjustment of this loop is described in Figure 4 and Kinemage 2.

Figure 4A shows the loop conformation in ricin A. A crystal contact with a symmetry-related molecule is indicated. This loop region is part of the molecular replacement test model and contributed to the initial phase set. There is only one hydrogen bond formed within the loop, between the amido nitrogen of residue 234 and the car-
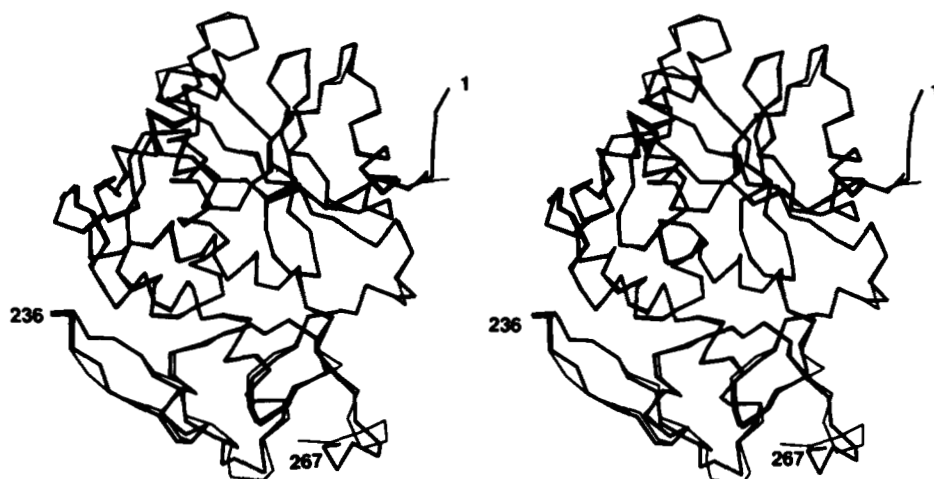
Fig. 2. Superposition of the refined models of ricin A and rRTA. Recombinant RTA, as refined in this study is shown in the heavy bonds as a Cα trace. The refined ricin A chain (Rutenber et al., 1991) is shown in thin bonds.

bonyl oxygen of 238. There are two additional hydrogen bonds formed with the neighboring B chain, one between the NH1 atom of Arg 234 of RTA and the carbonyl O of Val 141 of RTB and the other between the amido N of Arg 235 of RTA and the carbonyl O of the RTB terminal Phe 262. An additional contact is made between the amido N of residue 237 and carbonyl O of residue 4 of a symmetry-related RTA. Also shown are the important edge-to-face contacts with the aromatic rings of Phe 140 and Phe 262 of RTB and Phe 240 of RTA (Rutenber & Robertus, 1991). Figure 4B shows the rRTA conformation superimposed on the initial electron-density map for rRTA.

The process of refinement altered the loop as shown in Figure 4C. Compared to the ricin A chain model, two additional hydrogen bonds are formed in the loop (232 O with 240 N and 234 O with 237 N) making it an antiparallel β structure. In the ricin A chain model, the interatomic distances for these pairs of atoms are 3.8 and 4.0 Å, respectively. The refined rRTA model is shown superimposed on the final NED map in Figure 4D. Apparently contacts with RTB, which are strong in this portion

of the ricin A chain, and perhaps, to a lesser extent, crystal packing forces induce the distortions in the heterodimer structure. Release of RTB allows the structure to relax locally to a lower energy conformation. Unfortunately, we cannot determine from the crystal structure whether the release of the B chain or the differences in crystal packing forces are the predominant determinants of the local structural alteration.

In addition, there are minor differences between the two forms of A chain in other loop regions. These may be induced by the differing crystal packing and by the fact that ricin crystals are at pH 4.8 while rRTA is at pH 8.9.

An important question is what changes occur in the active site upon release of RTB? The two active sites are virtually superimposable as seen in Figure 5 and Kinemage 3. The subtle perturbation might be dismissed as reflecting differences in crystallization conditions. If so, the inactivity of heterodimeric ricin probably results from the physical constraints of the B chain interfering with ribosome recognition. The B chain does not block direct access to the catalytic site of RTA, at least for a small RNA ligand (Rutenber et al., 1991). It is important to remem-
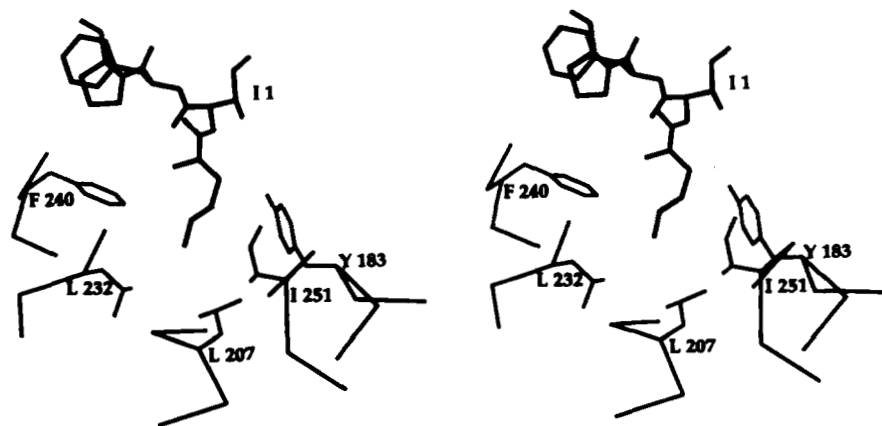

Fig. 3. Crystal packing buries Met 0 in a hydrophobic pocket. The rRTA expressed from *Escherichia coli* has an incompletely processed Met at the amino terminus; roughly 40% of the chains retain the initiator residue. The dark bonds indicate the amino-terminal residues 0–4 for a given rRTA. The side chain of Met 0 occupies a hydrophobic pocket on a symmetry-related molecule, shown in light bonds. This pocket is normally occupied by the side chain of Phe 262 from the B chain when the heterodimer is formed.
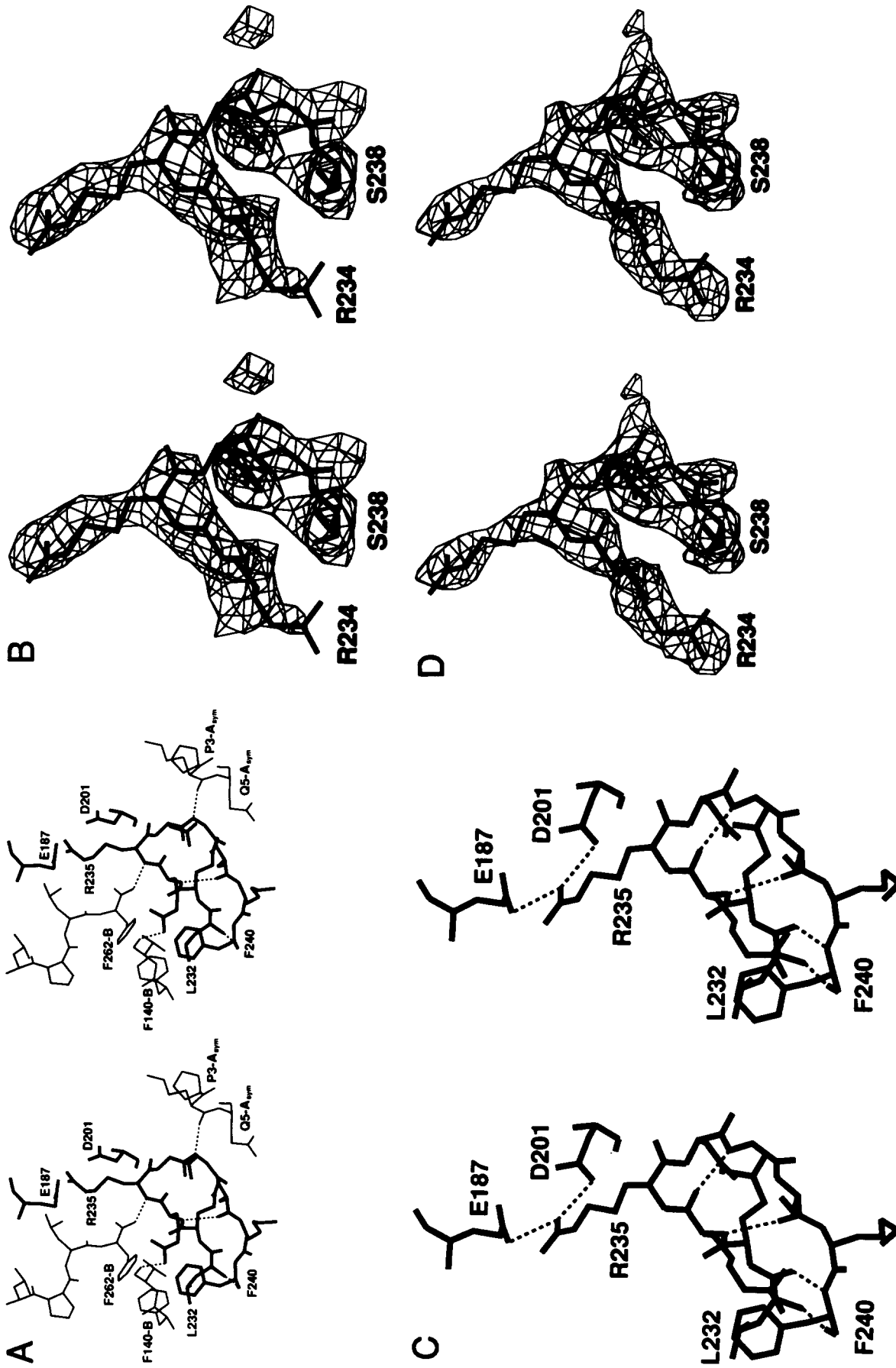
Fig. 4. Comparison of the conformation of a loop in the ricin heterodimer structure and in the rRTA structure. **A:** The loop (residues 232–240) as found in the heterodimer structure. The loop is shown with heavy bonds while parts of RTB and a symmetry-related RTA are drawn with light bonds. Possible hydrogen bonds are shown as dashed lines. **B:** The loop in the rRTA conformation is superimposed on the initial 2.5-Å NED map. The map has $2F_{obs,nat} - F_{calc}$ amplitudes and phases calculated from the ricin A model oriented in the rRTA cell. The contours enclose 15% of the cell volume. **C:** The loop structure in the refined rRTA structure. **D:** The final 2.5-Å NED map; 15% of the cell volume is enclosed by the contour.
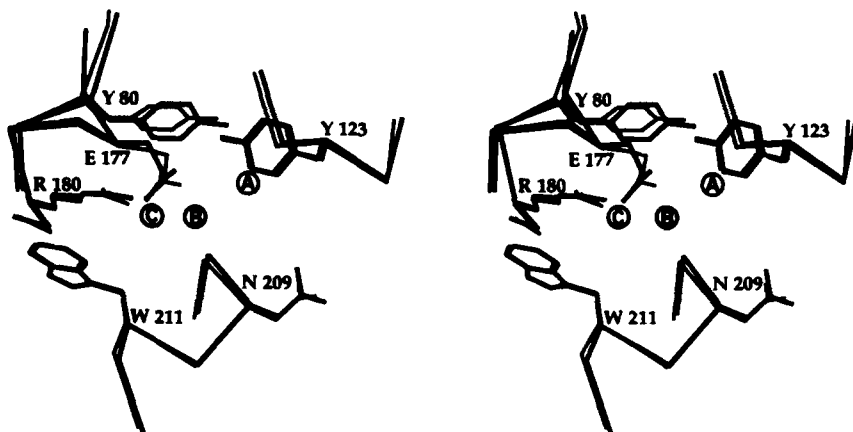
Fig. 5. The active site of ricin. The conformation of ricin A is shown in light bonds and that of rRTA in heavy bonds.

ber, however, that the ribosomal substrate is much larger than ricin and RTA may interact with it at places remote from the catalytic site. Indeed, we have speculated that nonspecific contacts might be made between RTA and the ribosome by ion pairs involving conserved Arg residues on the back side of RTA (Montfort et al., 1987). In short, the presence of B chain may interfere with RTA's normal recognition of the ribosomal landscape in ways that we presently do not understand in molecular detail.

The differences between ricin A chain and rRTA, however, are interesting in light of our recently proposed mechanism of action for RTA, based on the binding of substrate analogs (Monzingo & Robertus, 1992). The susceptible adenine ring of the substrate binds between Tyr 80 and Tyr 123, but Tyr 80 must rotate some 40° to accomplish this stacking. We see in Figure 5 that rRTA shows some movement in this direction although it has not moved to form the final aromatic pocket. Perhaps of greater importance is the water structure in the active site. Ricin A chain contains two waters, labeled A and B in Figure 5. These waters also exist in rRTA, although their centers shift very slightly. The rRTA structure also contains a new active-site water molecule, labeled C in Figure 5, and bonding to the crucial active site Arg 180. In proposing a mechanism for RTA, an RNA hexanucleotide model fitting the CGAGAG sequence attacked by ricin was fit to the active site (Monzingo & Robertus, 1992). It revealed a space that could accommodate a water molecule which was proposed to be bound by Arg 180 and activated as the ultimate nucleophile in the depurination reaction. One possibility was that water 323 (B in Fig. 5), seen in ricin A chain, might be moved into this position by substrate binding. We see, however, that rRTA already has a water bound in the proper position. The fact that this water, C, is present in RTA and absent in ricin may be due to a conformation rearrangement when RTB is released. More likely, the differences in pH of the ricin and rRTA crystals change the charge pattern in the active site and effect the water structure. Ricin crystals grow from 6% polyethylene glycol in acetate buffer at pH 4.75 (Vil-

lafranca & Robertus, 1977). The rRTA crystals grow from Tris buffer, pH 8.9, without any precipitating agent (Robertus et al., 1987). In either case, the structure of rRTA appears to better reflect the active geometry of this enzyme in that it provides an attacking water for the mechanism of action.

Materials and methods

Initially, recombinant RTA protein was obtained from Cetus Corporation as described in Robertus et al. (1987). An expression vector was also obtained from Cetus and engineered to express wild-type enzyme behind the β-galactosidase promoter, in a plasmid called pUTA (Ready et al., 1991). Wild-type protein was isolated from the expression of pUTA in *E. coli*, as described by Ready et al. (1991). Recombinant RTA was crystallized from low salt buffer, pH 8.9 in space group P2₁, with $a = 42.6$ Å, $b = 68.1$ Å, $c = 50.2$ Å, and $\beta = 112.9°$ as described in Robertus et al. (1987).

Three-dimensional diffraction data were collected to 1.9 Å resolution from wild-type rRTA crystals, using a San Diego Multiwire Systems area detector (Hamlin, 1985) and corresponding software (Howard et al., 1985). The X-ray source was a graphite-monochromatized GX-20 rotating anode generator operated at 40 kV, 40 mA. Data were reduced and potential derivatives evaluated as described in Montfort et al. (1987).

Over 40 heavy metal soaking conditions were tested in efforts to form isomorphous derivatives of rRTA; two showed weak but reproducible changes. Data were collected to roughly 2.5 Å resolution for a crystal soaked 5 weeks in a 1 mM solution of K_2PtCl_4. Data were also collected for a crystal soaked 4 weeks in a 2% saturated solution of adenine with methyl-mercury substituted at N9 (Me-Hg-adenine). This compound was synthesized by the method of Holy and Sorm (1969).

Rotation searches were performed using the fast-rotation function program of Tanaka (1977) and the MER-LOT package provided by Fitzgerald (1988). Translation

searches were also carried out using the MERLOT program suite. Rigid body refinement was done using CORELS (Sussman, 1985). Model building was done using the program FRODO (Jones, 1982) on an Evans and Sutherland PS390 graphics system. Crystallographic refinement of rRTA used the X-PLOR package, created by Axel Brunger (Brunger et al., 1987). The strategy of refinement was similar to that reported for the ricin heterodimer (Rutenber et al., 1991). We defined a round of refinement as a rebuilding, by hand, of the model followed by a variable number of cycles of automated refinement using the molecular dynamics option of X-PLOR on a CRAY Y-MP8/ **864.** The automated refinement used terms from **5** A to the nominal resolution limit of the run, typically 2.5 or **2.3** A.

At the end of each round of refinement a Fourier map was computed using the measured structure factor amplitudes and phases calculated from the newly refined model. As described previously (Rutenber et al., 1991), such a map is potentially biased by the calculated phases and so a NED map was calculated using an in house program, NEDFFT. A NED map is similar to an omit map except that a slab portion of the starting density is omitted and the remaining map is back-transformed to obtain new phases. These phases are then combined with the measured structure factor amplitudes to produce an unbiased slab of density, corresponding to that which was omitted. The process is repeated until the entire NED map is constructed. These maps have amplitudes of the form $(2F_{nat,obs} - F_{calc'})$, where the prime indicates that a portion of the model has been omitted. The maps were computed using terms from $10\text{\AA}$ to the nominal resolution of the map. Difference Fourier maps with amplitudes of the form $(F_{nat,obs} - F_{calc})$ and phases for the current model were also calculated to aid in rebuilding.

Acknowledgments

References

Brunger, A., Kuriyan, J., & Karplus, M. (1987). Crystallographic R factor refinement by molecular dynamics. *Science 235,* 458–460.

Bushnev, V. & Tonevitsky, A. (1989). High mobility of N-terminal parts of A and B subunits of ricin. *J. Biomol. Struct. Dyn. 6,* 1061–1070.

Endo, Y. & Tsurugi, K. (1988). The RNA *N*-glycosidase activity of ricin A-chain: The characteristics of the enzymatic activity of ricin A-chain with ribosomes and with rRNA. *J. Biol. Chem. 263,* 8735–8739.

Fitzgerald, P.M. (1988). MERLOT, an integrated package of computer programs for the determination of crystal structures by molecular replacement. *J. Appl. Crystallogr 21,* 273–278.

Frankel, A.E., Ed. (1988). *Immunotoxins.* Kluwer Academic Publishers, Boston.

Frankel, A., Welsh, P., Richardson, J., & Robertus, J.D. (1990). The role of arginine 180 and glutamic acid 177 of ricin toxin A chain in the enzymatic inactivation of ribosomes. *Mol. Cell. Biol. 10,* 6257–6263.

Halling, K.C., Halling, A.C., Murray, E.E., Ladin, B.F., Houston, L.L., & Weaver, R.F. (1985). Genomic cloning and characterization of a ricin gene from *Ricinus communis. Nucleic Acids Res. 13,* 8019–8033.

Hamlin, R. (1985). Multiwire area x-ray diffractometers. *Methods Enzymol. 114,* 416–452.

Holy, A. & Sorm, F. (1969). Preparation of some β-L-ribonucleosides. *Collect. Czech. Chem. Commun. 34,* 3383–3401.

Howard, A.J., Nielsen, C., & Xoung, N.H. (1985). Software for a diffractometer with multiwire area detector. *Methods Enzymol. 114,* 453–472.

IUPAC-IUB Commission on Biochemical Nomenclature. (1970). Abbreviations and symbols for the description of the conformation of polypeptide chains. *Biochemistry 9,* 3471–3479.

Jones, T.A. (1982). FRODO: A graphics fitting program for macromolecules. In *Computational Crystallography* (Sayre, D., Ed.), pp. 303–317. Oxford University Press, Oxford, UK.

Katzin, B.J., Collins, E.J., & Robertus, J.D. (1991). The structure of ricin A chain at 2.5 Å. *Proteins Struct. Funct. Genet. 10,* 251–259.

Kim, Y., Mlsna, D., Monzingo, A.F., Ready, M.P., Frankel, A., & Robertus, J.D. (1992). The structure of a ricin mutant showing rescue of activity by a noncatalytic residue. *Biochemistry 31,* 3294–3296.

Kim, Y. & Robertus, J.D. (1992). Analysis of several key active site residues of ricin A chain by mutagenesis and x-ray crystallography. *Protein Eng. 5,* 775–779.

Lamb, F.I., Roberts, L.M., & Lord, J.M. (1985). Nucleotide sequence of cloned cRNA coding for preproricin. *Eur. J. Biochem. 148,* 265–270.

Lord, J.M., Hartley, M.R., & Roberts, L.M. (1991). Ribosome inactivating proteins of plants. *Semin. Cell Biol. 2,* 15–22.

Montfort, W., Villafranca, J.E., Monzingo, A.F., Ernst, S.R., Katzin, B., Rutenber, E., Xuong, N.H., Hamlin, R., & Robertus, J.D. (1987). The three-dimensional structure of ricin at 2.8 Å. *J. Biol. Chem. 262,* 5398–5403.

Monzingo, A.F. & Robertus, J.D. (1992). X-ray analysis of substrate analogs in the ricin A chain active site. *J. Mol. Biol. 227,* 1136–1145.

Olsnes, S. & Pihl, A. (1982). Toxic lectins and related proteins. In *The Molecular Action of Toxins and Viruses* (Cohen, P. & Van Heynigen, S., Eds.), pp. 52–105. Elsevier Biomedical Press, New York.

Ready, M.P., Kim, Y., & Robertus, J.D. (1991). Site directed mutagenesis of ricin A chain and implications for the mechanism of action. *Proteins Struct. Funct. Genet. 10,* 270–278.

Robertus, J.D., Piatak, M., Ferris, R., & Houston, L.L. (1987). Crystallization of ricin A chain obtained from a cloned gene expressed in *Escherichia coli. J. Biol. Chem. 262,* 19–20.

Rutenber, E., Katzin, B.J., Collins, E.J., Mlsna, D., Ernst, S., Ready, M.P., & Robertus, J.D. (1991). The crystallographic refinement of ricin at 2.5 Å resolution. *Proteins Struct. Funct. Genet.* 10,240–250.

Rutenber, E. & Robertus, J.D. (1991). The structure of ricin B chain at 2.5 A resolution. *Proteins Struct. Funct. Genet. 10,* 260–269.

Sussman, J.L. (1985). Constrained–restrained least-squares (CORELS) refinement of proteins and nucleic acids. *Methods Enzymol. 115,* 271–302.

Tanaka, N. (1977). Representation of the fast-rotation function in a polar coordinate system. *Acta Crystallogr. A 33,* 191–193.

Villafranca, J.E. & Robertus, J.D. (1977). Crystallographic study of the anti-tumor protein ricin. *J. Mol. Biol. 116,* 331–335.

Vitetta, E.S. & Thorpe, P.E. (1991). Immunotoxins containing ricin or its A chain. *Semin. Cell Biol. 2,* 47–58.